Biomonitoring of dairy farm emitted ammonia in surface waters using phytoplankton and periphyton

Tulp, T.; Tietema, A.; Loon, E.E. van; Ebben, B.; Hall, R.L. van; Son, Mm. van; Barmentlo, S.H.

Science of the Total Environment 908 (2024) 168259

Contents lists available at ScienceDirect

Science of the Total Environment

journal homepage: www.elsevier.com/locate/scitotenv

Biomonitoring of dairy farm emitted ammonia in surface waters using phytoplankton and periphyton

Tamar Tulp [a], Albert Tietema [a], E. Emiel van Loon [a], Bram Ebben [a], Rutger L. van Hall [a], Michel van Son [a], S. Henrik Barmentlo [a,b,*]

[a] Institute for Biodiversity and Ecosystem Dynamics, University of Amsterdam, Science Park 904, 1090 GE Amsterdam, the Netherlands
[b] Institute of Environmental Sciences, Leiden University, 2300 RA Leiden, the Netherlands

HIGHLIGHTS

- Aim: Unravel the cattle stable – atmosphere - surface water - ecosphere ammonia pathway
- Environmental ammonia-N was regulated by the stable, and influenced by wind and rain.
- Atmospheric ammonia decreased from 43 to 6 μg/m^3 within 500 m from the stable.
- Aqueous ammonium reflected atmospheric NH_3, decreasing from 17 to 2 mg/L within 500 m.
- Periphyton and phytoplankton biomonitors captured atmospheric ammonia dynamics.

GRAPHICAL ABSTRACT

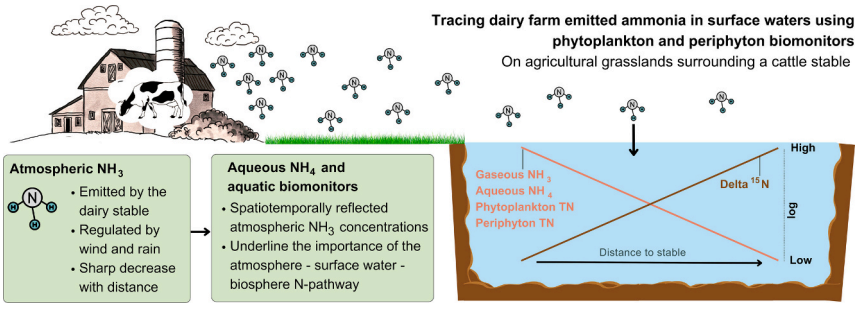

ARTICLE INFO

Editor: Sergi Sabater

Keywords:
Nitrogen
Isotopic composition
CN ratio
Eutrophication
Livestock farming
Biogeochemical flows

ABSTRACT

The increasing environmental abundance of reactive N ('Nr') entails many adverse effects for society such as soil degradation and eutrophication. In addressing the global surplus of N, there is a pressing need to quantify local sources and dynamics of Nr. Although quantified as an important anthropogenic source of Nr, the spatiotemporal patterns of ammonia ('NH_3') emitted by dairy farming and its resulting pressure on local surface waters lacks quantification. Quantification could optimize farm management with minimized losses of valuable nitrogen and protection of freshwater ecology. This study aimed to unravel spatiotemporal dynamics of ammonia nitrogen emitted by a dairy farm in the atmospheric and aquatic geo-ecosphere. Atmospheric NH_3 and aqueous ammonium ('NH_4^+') were determined over time, together with meteorological variables. Aquatic biomonitors (periphyton and phytoplankton) were employed to monitor the spatial impacts of cattle-stable emitted NH_3. Atmospheric NH_3 on the farm was significantly regulated by wind, sharply declining over increasing distances from the stable (average decrease in the dominant wind direction from 55.5 μg/m^3 at 20 m to 5.8 μg/m^3 at 500 m, in the other wind directions values decreased from 38.3 μg/m^3 to 6.0 μg/m^3). This was also reflected in local surface water concentrations of NH_4^+, with average concentrations decreasing from 37.0 mg [NH_4^+-N]/L at 65 m to 4.8 mg [NH_4^+-N]/L in the dominant wind direction, and from 1.2 to 0.7 in other directions. Periphyton biomass, total N ("TN") and $\delta^{15}N$ all significantly reflected spatiotemporal dynamics of atmospheric NH_3 and aqueous NH_4^+, as did phytoplankton TN. The cattle stable significantly influenced local water quality through atmospheric spreading of NH_3, and both aquatic biomonitors were influenced by and reflected dairy farm

* Corresponding author at: Institute for Biodiversity and Ecosystem Dynamics, University of Amsterdam, Science Park 904, 1090 GE Amsterdam, the Netherlands.
E-mail address: s.h.barmentlo@cml.leidenuniv.nl (S.H. Barmentlo).

https://doi.org/10.1016/j.scitotenv.2023.168259
Received 13 July 2023; Received in revised form 20 September 2023; Accepted 30 October 2023
Available online 7 November 2023

emitted NH_3 with a sharp dilution over distance. This study strongly underlines the importance of atmospheric transport of dairy farm emitted NH_3 and its effects on local water quality.

1. Introduction

Anthropogenic activities have greatly perturbed the biogeochemical cycles of nitrogen, an essential life-supporting element (Malagó and Bouraoui, 2021). Through activities such as artificial fertilizer production, there have been largescale increases in the environmental abundance of reactive nitrogen ('Nr') compounds (Humphreys et al., 2021), i.e. N-containing molecules that are more reactive and thus more readily biologically available (Galloway et al., 2003). Nowadays, roughly half of the world's population is dependent on food produced with nitrogen containing artificial fertilizers (Erisman et al., 2007). Because of this and other anthropogenic sources of Nr, the global amount of Nr in the environment has more than doubled in the last century, which is now considered one of the major drivers of biodiversity loss (Díaz-Álvarez et al., 2018). Examining the pathways through which Nr travels from atmosphere to biosphere, however, can be highly complex because of a diverse array of environmental interactions (De Vries et al., 2003; Nijssen et al., 2017). Reactive N can be deposited through wet- or dry deposition, meaning respectively that it either dissolves in rain, snow or fog or that it is deposited via airflow and then gaseous or aerosol exchange between atmosphere and organisms or soil or water (Díaz-Álvarez et al., 2018).

In the Netherlands in 2021, 65 % of all emitted Nr was NH_3, of which 54 % originated from cattle (predominantly dairy farming; Central Statistics Office (CBS), 2023a). Although being quantified as an important anthropogenic source of Nr, the spatiotemporal patterns of NH_3 emitted by dairy farming and its resulting pressure on local surface waters has not been quantified to a great extent (Ge et al., 2023). Most Dutch agricultural lands are intersected with networks of streams and ditches through which Nr can disperse (Oenema et al., 2005), and a considerable proportion of surface waters in the Netherlands experience eutrophication (Van Puijenbroek et al., 2014). For the protection of water quality and natural habitats, environmental monitoring of this Nr dispersal thus is crucial. Sensor-based quantification of atmospheric spread and deposition of Nr would theoretically be suitable for this, but it is practically impossible due its costs (Gökçe, 2016). Because of this, there is a need for effective methods to measure the spatiotemporal dispersal of Nr and its environmental impacts (Gökçe, 2016). Biomonitors and bioindicators appear to be promising methods for such type of environmental monitoring (Gökçe, 2016; Markert and Wünschmann, 2011). The term 'biomonitor' means: an organism that serves as a proxy for environmental chemical change, and 'bioindicator' means a species serving as an indicator for environmental change. Where bioindicators provide more qualitative (more relative) information, i.e. early warning signals of ecosystem changes, biomonitors provide (semi-) quantitative (more absolute) information of chemical changes (Díaz-Álvarez et al., 2018; Markert and Wünschmann, 2011). In addition, physiochemical analyses generally solely provide a snapshot of current conditions while biomonitors in-situ can also reflect ecosystem quality (Gökçe, 2016).

Periphyton is considered suitable for surface water biomonitoring of Nr loadings, it is highly responsive to changes in the aquatic environment, and already has been successfully implemented to detect differences in Nr loadings from anthropogenic sources (De Carvalho et al., 2020; Von Schiller et al., 2007). Periphyton is a microecosystem biofilm, consisting of a mixture of several algae, cyanobacteria, microbes, fungi etc., that can grow on artificial substrates, making it easy to sample (Azim et al., 2005; Wu, 2017). Furthermore, determining the stable isotope ratios of N within these biomonitors potentially allows for source tracing if the isotopic signature of the pollution source is different from that of the surrounding environment (Bedard-Haughn et al., 2003; Calizza et al., 2020; Choi et al., 2006; De Carvalho et al., 2020; Díaz-Álvarez et al., 2018; Elliott et al., 2018).

Phytoplankton are also considered suitable organisms for surface water biomonitoring (Gökçe, 2016). Their relatively short life cycles enable them to respond rapidly to environmental changes, yet they live long enough to represent long-term impacts. As autotrophic organisms, they occupy the boundary between habitat and the biotic environment. Featuring a rich diversity of species, each with unique environmental requirements, phytoplankton are broadly applicable for monitoring purposes. Increased growth is often observed as a result of Nr and phosphorus ('P') enrichment, rendering them eutrophication indicators (Gökçe, 2016; Maberly et al., 2022). They are potentially more sensitive to environmental changes due to their small size, and because they cannot migrate, they must either thrive or disappear. Their high spatial density renders them easy to sample.

To address the knowledge gap regarding the spatiotemporal dynamics of cattle stable emitted atmospheric NH_3 in the vicinity of dairy farms, this study determined atmospheric and aquatic ammonia nitrogen loadings, and employed aquatic biomonitors (periphyton and phytoplankton) at high spatial and temporal resolutions. The present farm was selected because is generally representative of the average Dutch dairy farm (in terms of size, soil and land use) in order to identify the potential presence and magnitude of the dairy stable - atmosphere - surface water - biosphere NH_3 pathway. To isolate the effect of the cattle stable, this study was conducted within a 500 m radius around the stable, where there were no other distinct sources of Nr. Firstly, we tested the hypothesis that the cattle stable regulates aqueous concentrations of NH_4^+ through NH_3 emissions from the stable and atmospheric distribution by wind. Second, we assessed how the biomonitors reflect the atmospheric NH_3 via investigating biomass, total N ('TN'), %N, and Chlorophyll A. We investigated the shifting $\delta^{15}N$ of the periphyton biomonitors over distance and time in order to investigate if the stable indeed acts as the main source of Nr. Ammonia that volatilizes from manure tends to have a more negative $\delta^{15}N$, i.e. a relatively higher amount of ^{14}N than naturally present in the surrounding environment (Calizza et al., 2020). We tested the hypotheses that the determined parameters of both periphyton and phytoplankton vary according to proximity to the stable and temporal atmospheric NH_3 loadings. At close proximity to the stable, we expected enriched biomass, total N and chlorophyll-a ('Chl-a') values, and lower $\delta^{15}N$ values.

2. Materials and methods

2.1. Site description

This study was conducted at a Dutch commercial dairy farm located in Friesland, the Netherlands (Fig. 1). Farm size and land use and land cover ('LULC') are representative of the average Dutch dairy farm. According to the Köppen-Geiger climate classification, this region has an oceanic climate (Cfb) (Beck et al., 2018). The climate is warm and temperate, with high amounts of precipitation and lack of a dry season. The farm is based on an oceanic clay deposit from the Holocene (representing a significant portion of the Netherlands), rendering it initially calceric (Nieuwenhuis and Schokking, 1997; Ritzema and Stuyt, 2015). In the past 20 years, on average there has been a prevailing southwestern wind (KNMI, 2023). The area predominantly consists of agricultural grassland (vegetated with *Lolium perenne* Linnaeus), with a cattle stable roughly in the middle. There is little potential obstruction that interferes with the spread of atmospheric NH_3. Other livestock farming practices are further than 1 km away from the stable, and there are no other interfering sources of Nr nearby. In total, the dairy farm

consists of approximately 250 cows, of which roughly 150 are lactating, which is similar in size of the local region average (i.e. 125 in the year 2022, Central Statistics Office (CBS), 2023b). Year-round, there are about 5–15 young cows in the stable to the west (Fig. 1). The cows were confined to the stable throughout the study period and were fed grass silage, corn, grain, hay, and supplements (i.a. 'Protiwanze' and 'Powerfood'). The annual milk production amounts to 2.088.512 kg (data for 2021). There is a total manure production of 5000 m^3/year, of which 72 % is used on- site. Most of the manure is collected in a large storage reservoir directly under the cattle stable. There was a small pile of straw containing manure directly next to the stable, which was moved south on the third sampling date (see Fig. 1). Southwest of the stable, a feedstock can be found for hay and feed concentrates. The cattle husbandries cover an area of about 2.7 ha. The general water flow direction in the research area was westward (usually <0.1 m/s, measured sporadically) and flow was blocked in several locations due to dead ends or barriers. Generally, the ditches had a width of three to four meters, the only distinct exceptions being SE5, SW4N, NW3 and NW4, which were between six and seven meters wide. All water bodies had a depth of 1 to 1.5 m.

2.2. Experimental design

At each sampling point atmospheric NH_3 was determined to assess its impact on changes in aqueous NH_4^+ and the biomonitors (Supplement Fig. 1). The sampling points were no further than 500 m around the stable to prevent interference from other farms (Fig. 1). Samples were collected with an interval of two weeks in the period between 4 August 2021 and 13 October 2021. Throughout the whole experiment, meteorological factors such as wind speed and direction, temperature, relative humidity, solar radiation and precipitation were recorded every 5 min using a Hobolink RX3000 meteo station situated at location NE2 (Fig. 1). Data was automatically stored and accessible online.

2.3. Atmospheric ammonia

Atmospheric NH_3 was determined using a passive sampler: 'ALPHA', purchased from the UK Centre for Ecology & Hydrology (Tang et al., 2017). The sampling container consisted of a supporting structure and container, a filter paper that was coated in citric acid to bind the NH_3, and a white PTFE (Teflon) membrane which protects the filter and restricts turbulence while allowing NH_3 to pass through. The supporting structure consisted of a wooden pole in the ground, with a cap that overarches the sampling containers (at a height of 1.5 m) to prevent disturbance from rain. The top of the cap also contained bird spikes, while the bottom contained Velcro tape to attach the sampling containers. In the case of sample loss (9/86 observations), the concentrations were estimated using a median decline coefficient, which have

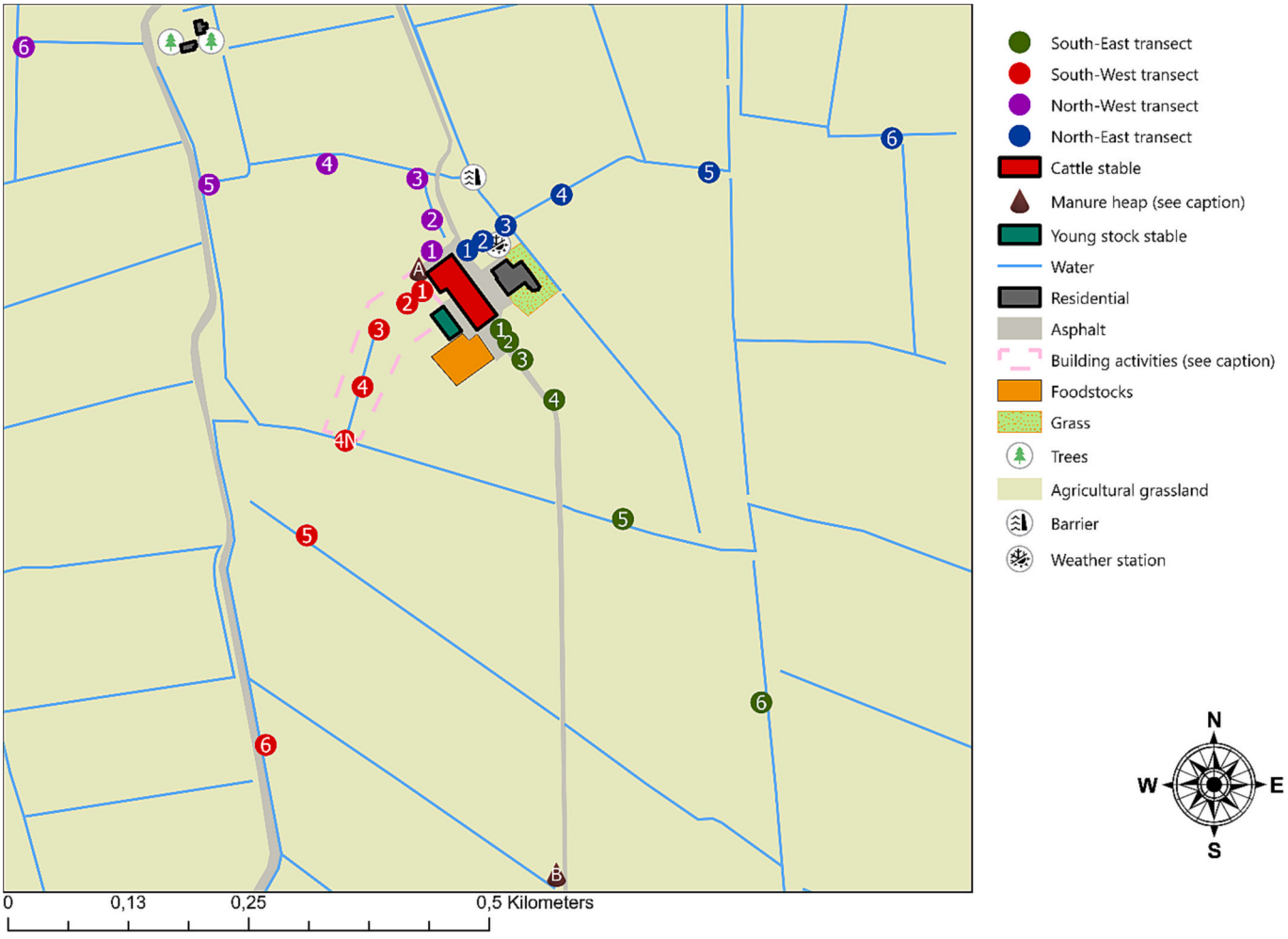

Fig. 1. Map of the research site with LULC and sampling locations. On the third (out of six) sampling moment of the experiment, the surface waters surrounded by dashed pink borders were backfilled. Therefore, the third SW sampling point was removed and the fourth migrated to the point listed as "4 N". Furthermore, the manure pile was then moved from A to B. The water flow direction in the ditches was westward. Location codes in the text are a combination of direction (indicated by the different colours) and the numbers in this map. The farm is located in the province of Friesland, the Netherlands.

been calculated for each sampling location using data from the past two years (Barmentlo et al., *in prep*).

To prepare the citric acid solution that was used to coat the filters, a fresh 120 g/L citric acid in methanol solution was prepared at each sampling moment. The coating solution was applied to the filters on ceramic dishes, the filters were subsequently put in a desiccator to dry. After sampling, the containers and samples were stored at 4 °C. The coated filters were then retrieved and placed in 10 mL deionised water for one hour, after which they were vigorously shaken by hand for 10 s to ensure that all the chemicals dissolved in the extractant and that the sample was well mixed. The filters were then removed from the solution and NH_4^+ concentrations in the solutions were analyzed using a Skalar SAN^{++} segmented flow analyser. The concentration of atmospheric NH_3 was calculated following the instructions by Tang et al. (2017).

2.4. Surface water chemistry

To collect the hydrological samples from which both surface water chemistry and phytoplankton contents were determined, five surface water samples were taken at approximately 10 cm depth. After collection, the samples were stored at −20 °C. After defrosting, the water samples were filtered using pre-weighed glassfiber Whatman GF/F filters (particle retention of 0.7 μm). The biological residue was later used to analyse phytoplankton contents (see 'Phytoplankton biomonitoring'). We then determined the concentrations of NO_2^-, NO_3^-, NH_4^+, TN, dissolved organic N and PO_4^{3-} in the filtrate using the segmented flow analyser. When values were below the detection limit (10 μmol/L for NH_4^+, PO_4^{3-} and total N or 'TN', and 3.5 μmol/L for NO_3) they were set to zero in further analysis.

2.5. Phytoplankton biomonitoring

The filters including the biological residue were stored in pre-weighed 3 mL Eppendorf tubes and then dried overnight in a freeze dryer to determine total dry weight per extraction volume (i.e. the biomass per volume sampled). In order to determine the C/N, the filters were subsequently ground to a homogeneous powder using a Bertin technologies bead beater (Precellys 24), weighed into tin boats and measured using an Elementar Vario EL cube elemental analyser. To adjust for the effect of the filters, we measured 12 blank filters that had the exact same treatment as the samples, except that demineralized water was filtered instead of surface water. The mean N value of these samples was subtracted from each individual sample.

Chlorophyll-a was determined using a Hydrolab HL7 OTT Hydromet, with a measuring interval of 1 s. The device was attached to a 1.7 m pole using a rope, and subsequently hung at a depth of approximately 10 cm for approximately 80 s, to enable the sensors to adjust to the environment. On the final sampling date, the Hydrolab malfunctioned. Instead, chlorophyll-a was measured in triplicate with an Aquafluor handheld fluorometer.

2.6. Periphyton biomonitoring

The periphyton was grown on 5 * 6 cm UV- permeable acrylic plates (Supplement Fig. 2), allowing biomass to accumulate over the measuring interval. The area designated for sampling the periphyton was 5 * 5 cm and was marked with a deep scratch in the plate. The residual 1 * 5 cm area was used to number the plates and attach the plates to an overhanging construction using a cable tie. The overhanging construction consisted of: (i) a rope bridging the surface water; (ii) a rope used to collect the sampler; (iii) a PVC pipe with nylon thread holding the samples; (iv) a steel pipe supporting the structure with its weight (Supplement Fig. 2). The construction was placed in the middle of the surface waters at each location. Every sampling moment, the plates were collected and swapped with clean plates. The plates were transported in plastic bags, and subsequently stored at −20 °C.

After thawing, the periphyton was scraped from the acrylic plates using a plastic putty knife to avoid scratching. The periphyton was subsequently collected in a measuring cup using tap water and then vacuum filtered through pre-weighed Whatman GF/C filters (particle retention of 1.2 μm). The filter and periphyton residue were stored in a pre-weighed 3 mL Eppendorf tube and then dried overnight in a freeze dryer to determine the dry weight. For each location (per sampling moment), biomass was determined for all six samples and three samples were subjected to isotope-ratio mass spectrometry analysis using an Elementar Vario EL cube elemental analyser coupled to an Elementar Bio Vision continuous flow isotope ratio mass spectrometer. Here the percentages of C and N were determined, together with the stable isotope ^{15}N:^{14}N ratio of the samples versus the atmospheric ^{15}N:^{14}N ratio, i.e. $\delta^{15}N$ (Bedard-Haughn et al., 2003). The $\delta^{15}N$ results were calibrated using USGS-25 and IAEA-N2, and the adjustment process for the impact of the filters for the EA-IRMS was equal to that of the EA (see 'Phytoplankton biomonitoring').

2.7. Statistical analyses

To account for locational differences and the repeated measures study design, we used linear mixed effect models to study the parameters affecting atmospheric NH_3 concentrations, surface water NH_4^+ concentrations, and the biomonitor variables (i.e. biomass, total N, $\delta^{15}N$, and Chlorophyll-a). The sampling location was chosen as random effect and time, direction, atmospheric NH_3 (where applicable) and distance as fixed effects. To examine the effects of wind and distance to the stable on atmospheric NH_3, we projected net wind vectors onto the vector between the stable and the measurement locations. To account for precipitation in the mixed-effect models, we integrated an interaction term between the total precipitation amount in the preceding two weeks and the count of data points with precipitation within that time period. Additionally, we also investigated the potential effect of ditch width, but this was insignificant for all scenarios and thus this variable was omitted from the results. The models were built using the 'nlme' package in R and were fitted using restricted maximum likelihood ('REML'). Models were built with a preferred maximum of two interactions, if the model assumptions were violated, a three- way interaction was applied. The best performing models were selected using an information- theoretic approach, via the 'dredge' function from the 'MuMIn' package based on the Bayesian information criterion ('BIC'), and Akaike information criterion ('AIC'). The models were subsequently evaluated for the assumptions: (i) that the response variable is a linear function of the fitted predictors; (ii) of homoskedasticity; (iii) of the absence of collinearity, using the 'performance' package in R; and (iv) of normality of residuals. Fixed effects were scaled and when assumptions were not met, a log transformation was applied to the response variable to ensure a better fit. Finally, the model statistics were reported using the 'anova.lme' function, with a 'marginal' sum of squares specification (Pinheiro and Bates, 2000).

3. Results

3.1. Geochemical parameters

There was a dominant southwestern wind throughout the experiment (Fig. 2); except during the third sampling moment when the dominant wind direction was north. There was relatively heavy precipitation at the start of the experiment (5.7 mm/day on average in the first month), followed by moderate rainfall in the following two months (1.3 and 1.9 mm/day, respectively; Supplement Fig. 3). Atmospheric NH_3 was always highest closest to the cattle stable (42.6 $\mu g/m^3$ on average at ~20 m) and sharply decreased with distance (on average 6.0 $\mu g/m^3$ at 500 m; Fig. 2). Atmospheric NH_3 values varied greatly between sampling moments and directions at a distance of roughly 20 m from the stable: (i) for the northeast direction, from 21.0 to 100.1 $\mu g/m^3$, the

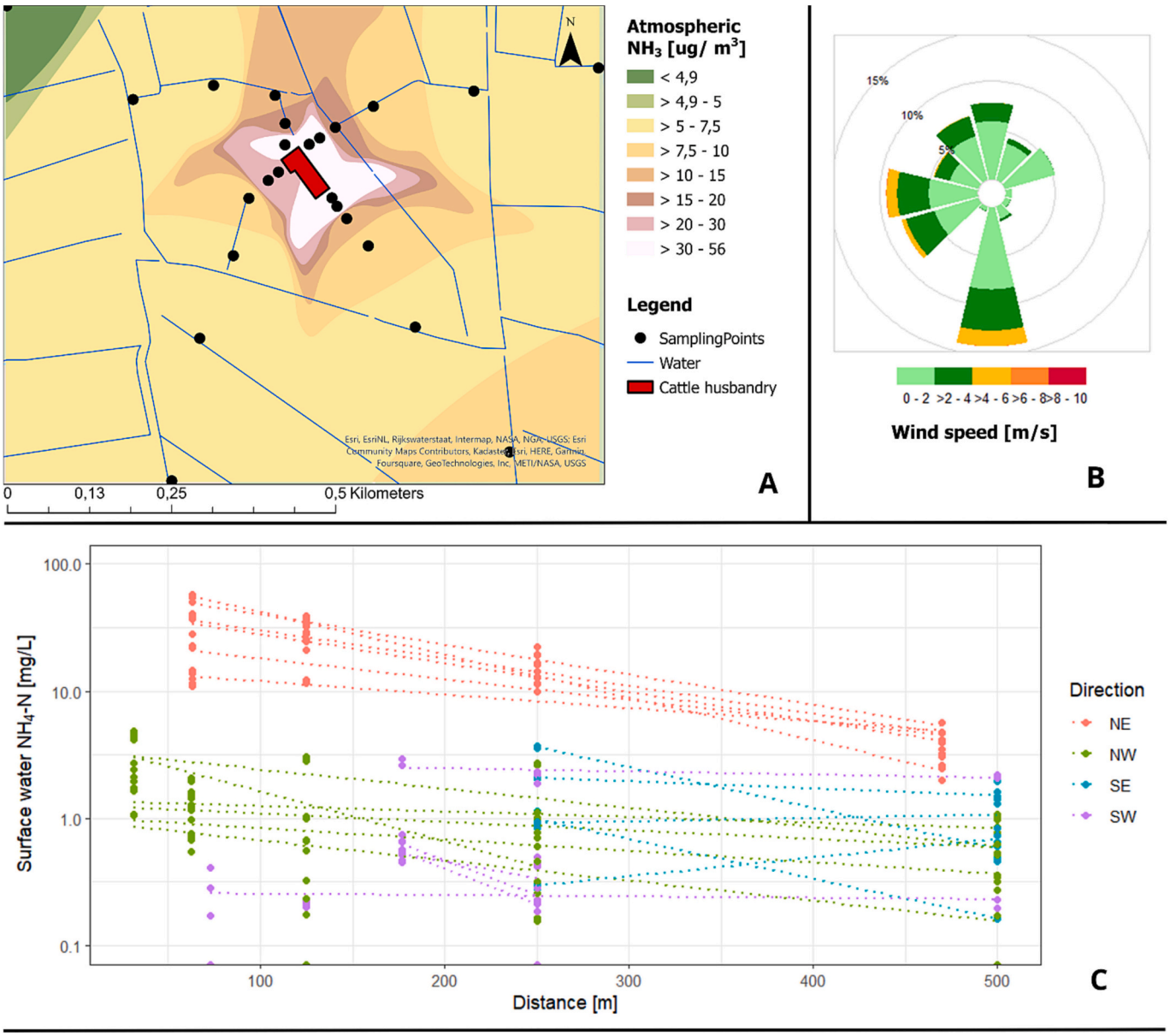

Fig. 2. Atmospheric NH_3 concentrations (A), wind rose (B) and surface water NH_4^+-N concentrations (mg/L) in relation to distance (m) to the stable (C) between 20 July 2021 and 13 October 2021. The atmospheric ammonia plot (A) was made by an Inverse Distance Weighing interpolation in ArcGIS pro 2.8. The wind rose shows where the wind originates from, and was constructed using data of the meteo station. The y-axis of plot (C) is displayed on a logarithmic scale. The different trendlines per wind direction indicate regression results from the six different time points (not coloured individually for visibility purposes). In (C): 'NE' = 'Northeast', 'SE' = 'Southeast', 'SW' = 'Southwest', 'NW' = 'Northwest'.

lowest being on day 29; (ii) in the northwest direction, values ranged between 6.6 and 56.7 $\mu g/m^3$, the lowest also being on day 29; (iii) between 33.5 and 108.7 $\mu g/m^3$ for the southeast direction; and (iv) for the southwest direction, between 7.5 and 36.7 $\mu g/m^3$. Observed ranges of NH_3 concentrations displayed temporal variability, with peaks on the first and fourth sampling moments, and lower values on the third and final periods (Supplement Fig. 3). Atmospheric NH_3 was significantly positively associated with the wind vector projections in the direction of the sample ($F_{1,115} = 30.01$, $p < 0.001$), and negatively associated with the effects of distance ($F_{1,22} = 27.27$, $p < 0.001$) and time ($F_{1,115} = 9.80$, $p = 0.002$). Importantly, there was a significant interaction between precipitation and the count of timepoints that had precipitation ($F_{1,115} = 85.28$, $p < 0.001$; Supplement Table 1).

Generally, surface water concentrations of NH_4^+ decreased with distance and were within close range of each other for the different directions at 500 meters distance to the stable, with concentrations for the northeast direction being roughly a factor 6 higher (3.7 mg [NH_4^+-N]/L vs 0.6 mg [NH_4^+-N]/L on average at 500 m). Surface water concentrations of total nitrogen ('TN') were predominantly dominated by N from NH_4^+ (median of 55 %) and were continuously highest close (≤65 m) to the stable (ranging from 2 to 57 mg [TN]/L or 0 to 54.0 mg [NH_4^+-N]/L, depending on the sampling date). Concentrations of NH_4^+ were on average a factor of 31 higher in the northeast direction compared to the other directions at a distance of 65 m from the stable (28.7 mg [NH_4^+-N]/L compared to 0.9 mg/L). Concentrations of surface water NH_4^+ were significantly associated with atmospheric NH_3 ($F_{1,225} = 20.78$, $p < 0.001$), time of sampling ($F_{1,225} = 48.28$, $p < 0.001$) and an interaction between direction and distance ($F_{3,8} = 5.21$, $p = 0.028$; Table 1). An example of when atmospheric NH_3 was markedly influential on surface water NH_4^+ is on sampling moment six, when concentrations in the northwest direction were higher than on the previous sampling moment (2.6 vs 1.3 mg [NH_4^+-N]/L), after atmospheric NH_3 values in the

Table 1
Mixed effect model results for the response variables surface water ammonium, periphyton $\delta^{15}N$ and TN, and phytoplankton TN. The marginal R^2 (R^2m) and conditional R^2 (R^2c) are listed per model.

	Geochemical				Periphyton					Phytoplankton			
	Surface water ammonium[a] (R^2m: 0.87, R^2c: 0.92)				$D^{15}N$ (R^2m: 0.51, R^2c: 0.83)				Total N[b] (R^2m: 0.61, R^2c: 0.75)				Total N[b] (R^2m: 0.50, R^2c: 0.53)			
	numDF	denDF	F.value	p.value	numDF	denDF	F.value	p.value	numDF	denDF	F.value	p.value	numDF	denDF	F.value	p.value
Gaseous NH_3	1	225	20.780	<0.001	1	164	11.059	0.001	1	159	3.463	0.065	1	209	6.105	0.014
Day	1	225	48.278	<0.001	1	164	1.332	0.250	1	159	22.717	<0.001	1	209	3.003	0.085
Direction	3	8	58.637	<0.001	3	12	17.452	<0.001	3	12	6.655	0.007	3	8	22.834	<0.001
Distance	1	8	32.519	<0.001	–	–	–	–	–	–	–	–	1	8	21.191	0.002
Direction * Distance	3	8	5.208	0.028	–	–	–	–	–	–	–	–	3	8	6.887	0.013
Gaseous NH_3 * Day	–	–	–	–	1	164	13.637	<0.001	–	–	–	–	–	–	–	–
Gaseous NH_3 * Direction	–	–	–	–	–	–	–	–	3	159	4.783	0.003	3	209	4.482	0.005
Day * Direction	–	–	–	–	–	–	–	–	3	159	17.498	<0.001	3	209	5.773	0.001
Gaseous NH_3 * Distance	–	–	–	–	–	–	–	–	–	–	–	–	1	209	2.372	0.125

[a] A log (X + 1) transformation was applied to the response variable.
[b] A log transformation was applied to the response variable.

previous two weeks were high in that location (27.7 μg/m^3). Aqueous NH_4^+ values displayed temporal variability, e.g. for the northeast direction, values increased in the first three sampling moments, followed by decreasing values in the consecutive sampling moments, with a final peak on the final two sampling moments (Supplement Fig. 3). A positive correlation between aqueous NH_4^+ and PO_4^{3-} concentrations was found for all sampling dates: (i) $|\rho| = 0.82$, $p < 0.0001$; (ii) $|\rho| = 0.77$, $p < 0.0001$; (iii) $|\rho| = 0.85$, $p < 0.0001$; (iv) $|\rho| = 0.90$, $p < 0.0001$; (v) $|\rho| = 0.76$, $p < 0.0001$; (vi) $|\rho| = 0.69$, $p < 0.0001$, respectively. For PO_4^{3-} concentrations, dissolved oxygen levels and pH values, see 'Supplement Table 2'.

3.2. Biomonitor assays

3.2.1. Periphyton

Periphyton TN values were on average a factor of 183 higher in the northeast direction (0.29 g[N]/m^2 on average) than in the other directions (<0.01 g[N]/m^2 on average), at distances below 180 m to the stable. The effect of surface water NH_4^+ on TN had an interaction with the sampling direction ($F_{3,163} = 3.80$, $p = 0.011$). Total N values decreased with distance, but TN values in the northeast direction kept exceeding the other directions at any given distance. Surface water NH_4^+ concentrations were positively related with TN values (Fig. 3). Periphyton TN was significantly influenced by interactions between atmospheric NH_3 and sampling direction ($F_{3,159} = 4.78$, $p = 0.003$) & time of sampling and direction ($F_{3,159} = 17.50$, $p < 0.001$). Reported TN values varied over time of sampling, e.g. the average maximum values that were found were a factor of 22 higher on the third sampling moment (1.06 g[N]/m^2) compared to sampling moment five (0.05 g[N]/m^2).

Similar to the results for TN, periphyton biomass was highest in the northeast direction, at the two points closest to the stable (63 and 125 m from the stable). Periphyton biomass was significantly reflective of a three-way interaction between atmospheric NH_3, time and direction ($F_{3,336} = 16.53$, $p < 0.001$), and interactions between time and distance & direction and distance ($F_{1,336} = 12.95$, $p < 0.001$; $F_{3,8} = 4.82$, $p = 0.03$, respectively; Supplement Table 1). Observed periphyton biomass values generally decreased with distance. On average, periphyton biomass was a factor 12 higher in the northeast direction compared to points in other directions, at distances under 180 m from the stable (8.4 vs. 0.7 g/m^2), these values decreased with distance to values slightly above the other directions (on average, 3.5 compared to 1.3 g/m^2 at ~500 m from the stable) Time was also highly influential, at these same locations, average values of periphyton biomass varied between 3.0 and 17.2 g/m^2, depending on the sampling date. Percentages of N in Periphyton, and hence C/N ratios, followed similar patterns as periphyton TN, the prior yielded similar model structures (Supplement Table 1).

Surface water concentrations of NH_4^+ were significantly negatively associated with $\delta^{15}N$ values ($F_{1,166} = 20.60$, $p < 0.001$; Supplement Table 1) and $\delta^{15}N$ values were consistently lowest in the northeast direction, for all distances and timepoints (on average − 1.31 ‰ compared to 3.80 ‰ on average for other directions; Fig. 4). Periphyton $\delta^{15}N$ was significantly affected by an interaction between atmospheric NH_3 values and time ($F_{1,164} = 13.64$, $p < 0.001$; Table 1), and the sampling direction ($F_{3,12} = 17.45$, $p < 0.001$). For example, on the final sampling moment atmospheric NH_3 concentrations were among the highest that were encountered in this study (on average 29.7 μg/m3) while $\delta^{15}N$ values of the point north of the stable (NW2; Fig. 1) were remarkably lower than previous sampling moments (−1.60 ‰ vs 5.52 ‰ at NW2).

3.2.2. Phytoplankton

As for the phytoplankton measurements, TN was significantly related to aqueous NH_4^+ concentrations ($F_{1,217} = 29.31$, $p < 0.001$), and decreased with distance, where values at the highest distance were within close range of each other irrespective of wind direction (0.01 to 0.40 mg/L). Phytoplankton TN was also highest for the northeast

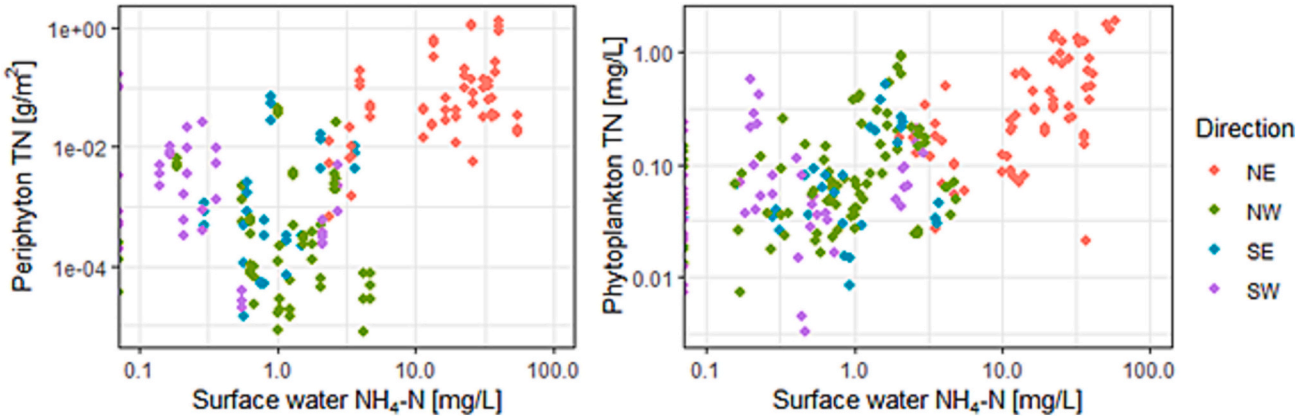

Fig. 3. Periphyton TN (left)- and Phytoplankton TN (right) versus surface water ammonium concentrations, per wind direction. The figures contain all observations (i.e. entire measurement period and all sampling locations). All axes were displayed on logarithmic scales. 'NE' = 'Northeast', 'SE' = 'Southeast', 'SW' = 'Southwest', 'NW' = 'Northwest'.

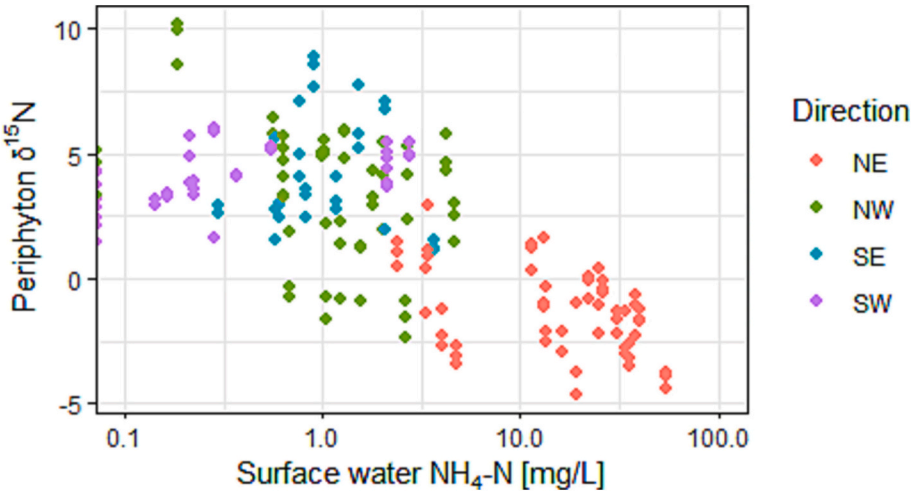

Fig. 4. Periphyton $\delta^{15}N$ versus surface water NH_4^+-N concentrations. Values from six sampling moments have been plotted, with an interval of two weeks in the period between 4 August 2021 and 13 October 2021. The figure contains all observations. 'NE' = 'Northeast', 'SE' = 'Southeast', 'SW' = 'Southwest', 'NW' = 'Northwest'. Aqueous NH_4^+-N values are displayed on a logarithmic scale.

direction (Fig. 3); ranging from 0.10 to 1.73 mg/L at 65 m distance to the stable compared to values between 0.04 and 0.77 mg/L at the same distance for the other directions. We found that direction, distance to the cattle stable, atmospheric NH_3 and time all significantly influenced phytoplankton TN, through a variety of interactions (Table 1); the most important ones being: (i) direction by distance ($F_{3,8} = 6.89$, $p = 0.013$); (ii) atmospheric NH_3 by sampling direction ($F_{3,209} = 4.48$, $p = 0.005$); and (iii) day by direction ($F_{3,209} = 5.77$, $p = 0.001$). Phytoplankton %N displayed similar patterns as TN, and the same fixed effect model structures best fitted the data according to the 'dredge' analysis (see 'Statistical analyses'; Supplement Table 1). Phytoplankton biomass did not reflect noticeable spatial patterns.

The effect of atmospheric NH_3 on Chl-a values did not contribute to the best model fit as observed from the 'dredge' results (see 'Statistical analyses'). Surface water NH_4^+ concentrations were significantly related to Chl-a, through an interaction with sampling moment ($F_{1,67} = 5.19$, $p = 0.026$), furthermore, the interaction between direction and distance was significant ($F_{3,8} = 4.81$, $p = 0.034$). At 65 m from the stable, Chl-a was highest for the northeast direction in five out of six cases (25 to 103 μg/L, compared to 12 to 60 μg/L in the other directions). At higher distances from the stable, the patterns of Chl-a displayed high variation among sampling locations and between sampling moments, the exception being the northeast direction, where Chl-a concentrations decreased with distance. For the final sampling date (when a different methodology was used for Chl-a measurements, see '*Phytoplankton biomonitoring*'), there were very distinct patterns where Chl-a started enriched and decreased with distance. For this timepoint, there was a high positive correlation between aqueous NH_4^+ concentrations and Chl-a values, with Spearman $|\rho| = 0.89$, $p < 0.001$.

4. Discussion

We aimed to assess the spatiotemporal dynamics of atmospheric and aqueous NH_3 emitted by a dairy stable using phytoplankton and periphyton biomonitors. We found that atmospheric NH_3 on the farm differed over time, was strongly regulated by wind projections, and declined sharply with increasing distances to the stable. This had profound effects on Nr dynamics in surface waters since we observed coinciding biomonitor responses where atmospheric NH_3 concentrations were high.

4.1. Geochemical parameters

Analysis revealed that atmospheric NH_3 was significantly associated with wind projections in the direction of the sample, originating from the stable (in the prior two weeks), distance to the stable, precipitation

and time. The fact that cardinal direction did not attribute to the best model fit, reinforces that observed atmospheric NH_3 loadings predominantly originated from the stable. Observed spatial dynamics of atmospheric NH_3 are consistent with common literature such as Shen et al. (2016), who observed that NH_3 concentrations decreased exponentially with distance away from a cattle feedlot. The regulatory role of temperature and precipitation for NH_3 levels was also observed by Hickman et al. (2021). The patterns of aqueous concentrations of NH_4^+ were significantly affected by atmospheric NH_3, indeed supporting our first hypothesis that aqueous concentrations of NH_4^+ are regulated by NH_3 emissions to the stable and distribution by wind.

Aqueous NH_4^+ concentrations were consistently highest in the northeast direction of the stable, following the predominant wind direction as measured throughout the experiment. For temperate species, species sensitivity modelling based on chronic toxicity data indicates that 95 % of species is protected at <2.6 mg/L total ammonia N (95 % confidence interval: 0.7 to 4.7; 5 % hazardous concentration 'HC5') (Mooney et al., 2019). In the present study, aqueous NH_4^+-N concentrations in the northeast direction exceeded this HC5 ecotoxicological threshold at any given distance and sampling moment, by a factor 1.4 at 500 m and 11.0 at 63 m (NH_3-N excluded); stressing the impact of dairy farming on local water quality. In the other wind directions, HC5 ecotoxicological thresholds were transgressed in 11 % of all cases, mainly in the northwest direction. According to Camargo and Alonso (2006), eutrophication typically occurs with TN values above the 0.5–1.0 mg/L range; in the present study, all reported TN values were higher than 0.7 mg/L, 89 % of all observations being higher than 1.0 mg/L. While observed TN values mainly consisted of NH_4^+, concentrations of other forms of Nr (dissolved organic N, NO_2 and NO_3) amounted to a median of 1 mg [N]/L, which are likely mainly attributed to nitrification and leaching.

In assessing aqueous dynamics of Nr, it is important to consider water flows within the catchment and legacy effects (Martin et al., 2016; Schulte-Uebbing et al., 2022). For instance, water flow was haltered by a barrier in the northeast direction (Fig. 1). This, together with the observed dilution of Nr away from the stable (the only distinct point source in the vicinity), suggests that the eutrophic state of these surface waters likely reflected the effect of long-term exposure to enhanced Nr deposition with limited discharge. Degrees of eutrophication were thusly high in this location that the nutrient-regulating capacity of the ditch ecosystem appeared to be strongly hampered (as was also reflected by the local PO_4^- concentrations, that ranged from 6 to 37 mg/L); this is further supported by our personal observations of notably sparse biota (other than algae and periphyton) in this area. The prevailing southwestern wind likely further enhanced the observed hotspot in the northeast. Another potential source of Nr here could be fertilization with manure, but all farming practices (including manure application and artificial fertilizer) were equal between plots. Furthermore, the present soil was mostly clay (see 'Methods - Site description'), which potentially also limited the loss of Nr via leaching. This is supported by the fact that NO_3^- concentrations were below the detection limit in 86 % of all cases, and leached Nr is mainly in this form (Yu et al., 2007).

4.2. Biomonitor assays

Perceived enrichments in both atmospheric NH_3 and aqueous NH_4^+ corresponded strongly with the tested aquatic biomonitors; they significantly reflected the spatial and temporal impacts of the cattle stable, i.e. via continuous atmospheric NH_3 loading and thus deposition (Table 1). We found that the atmospheric NH_3 significantly impacted nearly all biomonitor parameters measured since biomass, TN, %N and $\delta^{15}N$ all reflected the local air concentrations where chlorophyll-a did not. Worth noting is that biomonitor growth did not seem limited by PO_4 concentrations. The most Nr enriched sites displayed the highest algal biomass, which is consistent with previous research listing extreme algal blooms as indicators for excess nutrients (Gökçe, 2016; Maberly et al., 2022; Toda et al., 2002). Interestingly, wind direction was of significant importance for all parameters, reflecting the prevailing wind direction. However, the listed biomonitors and parameters had a different magnitude of response to N deposition. For example, periphyton biomass was more reflective of sites that received the highest loadings of NH_3. This is consistent with research by Von Schiller et al. (2007), who found that NH_4^+-N was the preferred N-source of periphyton. This, coupled with its low labour requirements, renders it a promising biomonitor to determine extreme environmental loadings of NH_4^+. For more quantitative information, the same sample (or phytoplankton) could be subjected to further elemental analysis; we found that periphyton- and phytoplankton TN were also highly reflective of: (i) the spatial relation to the stable, i.e. distance, wind direction and NH_3 loading; and (ii) surface water concentrations of NH_4^+. In the most polluted site (NE3), periphyton TN values were a striking factor of 183 higher (0.29 g[N]/m^2 on average) compared to the other directions at the same distances (<0.01 g[N]/m^2 on average). The substantial TN values are the result of the fact that both biomass and %N values were high at locations with higher Nr concentrations. Overall, this study shows that phytoplankton and periphyton can act as suitable biomonitors for local atmospheric NH_3 dynamics. Since our analyses already showed a significant impact of time within a timeframe of ten weeks during the final stage of summer and start of autumn, and the fact that growth will likely vary greatly across the seasons (Oishi, 2023), an interesting development could be to look more closely at the temporal dynamics of N in the assessed biomonitors.

Where growth and nutrient contents of periphyton and phytoplankton are typically influenced by external factors such as temperature and light (Zhao et al., 2017), $\delta^{15}N$ mainly depends on the isotopic signature of the source of the Nr (Díaz-Álvarez et al., 2018). While isotopic spatial gradients (or 'isoscapes') are generally accepted as effective tools to characterize biogeochemical gradients on larger scales (Vokhshoori and McCarthy, 2014), the results of this study show that $\delta^{15}N$ is suitable for tracing atmospheric NH_3 dynamics in small-scale spatial and temporal resolutions, when there is a point source with a distinct isotopic signature. Periphyton δ15N was found to be highly responsive to sudden environmental changes, e.g. for the northwest direction on the sixth sampling moment, when the δ15N of site NW2 greatly decreased compared to the previous sampling moment after extreme NH3 inputs from the stable, exposing a clear gradient of spatial impact. The $\delta^{15}N$ values in this study were always lowest at sites with the highest aqueous and atmospheric NH_x concentrations which is consistent with Finlay and Kendall (2007), who found that $\delta^{15}N$ values in surface waters ranges between −1 and +7 ‰ in pristine sites, compared to −15 to +20 ‰ in polluted sites. Our findings are also in agreement with Calizza et al. (2020) and De Carvalho et al. (2020), who observed similar ranges in $\delta^{15}N$ for inorganic pollution originating from agriculture. A major challenge in the utilization of $\delta^{15}N$ for quantifying spatial impacts of farms can however be the difference between isotopic signatures of atmospheric NH_3 distribution, which depletes the $\delta^{15}N$, and fertilization with manure, which increases the $\delta^{15}N$ (De Carvalho et al., 2020). In our study, we found no such interference, indicating that this effect can be limited if stable emissions are relatively high versus unintended Nr losses from manure application (through e.g. runoff and leaching).

4.3. Towards integrated management

The distinct enrichment of surface water NH_4^+ via atmospheric environmental loadings in the present study highlights the importance of integrating both local hotspots of aqueous Nr and meteorological dynamics in: (i) the assessment of spatial impacts of Nr emissions; (ii) spatial planning; (iii) policy making; and (iv) the formulation of mitigation strategies. In this study, at 500 m from the stable, the HC_5 was mostly transgressed in the northeast direction, indicating the relative importance of spatiality of a given dairy farm. Hence, besides proximity between Nr emitters and nature reserves, wind direction and aquatic

streams should also be considered in farm layout planning. In unravelling the dynamics of atmospheric NH_3 concentrations, terrestrial- and aqueous Nr and legacy effects, it will also be crucial to determine the factors regulating the bi-directional transport of NH_3 between surface waters and air (Bleeker, 2018). In safeguarding the biogeochemical cycles, Schulte-Uebbing et al. (2022) call for coordinated action, which integrates the heterogeneity of site-specific Nr sources, surpluses and vulnerabilities. In achieving this, it will be crucial to quantify small-scale dynamics of Nr in a swift, integrative and economically responsible manner. The results of this study suggest that aquatic biomonitors are promising agents to do so in order to investigate aqueous transport and impacts. It is recommended to research the most suitable biomonitors to enable: (i) optimized farm management with minimized surpluses, by addressing the relationships between atmospheric NH_3 concentrations, legacy effects and aqueous Nr concentrations; (ii) apt identification of peak Nr fluxes, in its different forms (e.g. NH_4^+, NH_3, NO, NO_2, and NO_3^-); and (iii) multi-element biomonitor and bioindication methods, fitted to the requirements- and emissions of different sites.

Our findings generate valuable insights into how various factors such as wind direction, temperature, and precipitation affect the stable - atmospheric NH_3 – aqueous NH_4 – aquatic biota pathway at the local scale. Worth noting is that site- specific factors such as aquatic streams, obstructions that affect air flows and variations in the geo-ecosphere might affect the aforementioned pathway. Unravelling how this pathway is affected by aforementioned factors is recommended to develop tailored strategies. However, the mechanisms, processes and biomonitor responses observed at this farm (such as the effects of wind direction, temperature, and precipitation on Nr dispersion, or the effect of NH_3 on periphyton growth) are not unique to this specific setting, making our results valuable for understanding broader patterns. These local studies are critical for informing larger scale studies and strategies, especially given that one-size-fits-all approaches can overlook local peculiarities that could be key to effective nitrogen management.

5. Conclusions

In this study, we used aquatic biomonitors (periphyton and phytoplankton) to address the spatiotemporal dynamics and impacts of ammonia nitrogen surrounding cattle stable. We found that the stable significantly regulated both atmospheric NH_3 concentrations and surface water concentrations of NH_4^+, this was reflected in biomonitor biomass, TN and $\delta^{15}N$ composition. Due to the prevailing southwestern wind and legacy effects, there was a dominant loading of aqueous NH_4^+ that exceeded the ecotoxicological HC5 threshold in 35 % of all observations. This environmental accumulation of Nr also resulted in severe eutrophication of the surface water. Importantly, we found that all measured biomonitor variables were both spatially and temporally reflective of NH_3 emitted by the dairy stable and that all observed heightened environmental total ammonia nitrogen loadings decreased sharply with distance. Our study thus underlines the significant influence and strong distance-related effect of dairy farming on local water quality via atmospheric transport of NH_3 while also indicating the relative importance of this pathway. While focused on a single farm, this study sheds light on universal mechanisms that regulate a perhaps overlooked ammonia pathway, offering invaluable insights that can inform targeted, locally sensitive approaches and studies for more effective nitrogen management on a broader scale.

CRediT authorship contribution statement

T.T., S.H.B., E.E.L A.T. conceptualized the experiment; T.T., S.H.B., B.E., R.L.H. and M.S. gathered and analyzed the samples; T.T., S.H.B. and E.E.L. analyzed the data; T.T. and S.H.B led the writing of the manuscript; all authors contributed to the interpretation of the data, writing of the MS and gave final approval for publication.

Declaration of competing interest

The authors declare no conflict of interest.

Data availability

Data will be made available on request.

Acknowledgements

This project was funded by the foundation Mesdag-Zuivelfonds NLTO. We are grateful to Saskia Wijlhuizen, Sasja Tulp, Sam Beukers, Mees Wortelboer, Victor Jourdain, Claudia Schwennen and Jasmijn van Gool for helping with the measurements. We thank Martina Vijver (Leiden University) for providing the handheld fluorometer.

Appendix A. Supplementary data

Supplementary data to this article can be found online at https://doi.org/10.1016/j.scitotenv.2023.168259.

References

Azim, M.E., Beveridge, M.C.M., Van Dam, A.A., Verdegem, M.C.J., 2005. Periphyton and aquatic production: an introduction. In: Periphyton: Ecology, Exploitation and Management. CABI Publishing, pp. 1–13.

Beck, H.E., Zimmermann, N.E., Mcvicar, T.R., Vergopolan, N., Berg, A., Wood, E.F., 2018. Data descriptor: present and future Köppen-Geiger climate classification maps at 1-km resolution. Nat. Sci. Data 5. https://doi.org/10.1038/sdata.2018.214.

Bedard-Haughn, A., Van Groenigen, J.W., Van Kessel, C., 2003. Tracing 15 N through landscapes: potential uses and precautions. J. Hydrol. (Amst.) 272, 175–190. https://doi.org/10.1016/S0022-1694(02)00263-9.

Bleeker, A., 2018. Quantification of Nitrogen Deposition and Its Uncertainty With Respect to Critical Load Exceedances. VU, Amsterdam.

Calizza, E., Favero, F., Rossi, D., Careddu, G., Fiorentino, F., Sporta Caputi, S., Rossi, L., Costantini, M.L., 2020. Isotopic biomonitoring of N pollution in rivers embedded in complex human landscapes. Sci. Total Environ. 706 https://doi.org/10.1016/j.scitotenv.2019.136081.

Camargo, J.A., Alonso, Á., 2006. Ecological and toxicological effects of inorganic nitrogen pollution in aquatic ecosystems: a global assessment. Environ. Int. 32, 831–849. https://doi.org/10.1016/j.envint.2006.05.002.

Central Statistics Office (CBS), 2023a. Stikstofemissies naar lucht [WWW Document]. URL. https://www.cbs.nl/nl-nl/dossier/dossier-stikstof/stikstofemissies-naar-lucht#:~:text=Het%20wegverkeer%20heeft%20met%2033,aandeel%20van%20ongeveer%2012%20procent. (Accessed 8 July 2023).

Central Statistics Office (CBS), 2023b. Landbouw; gewassen, dieren, grondgebruik en arbeid op nationaal niveau [WWW Document]. URL. https://opendata.cbs.nl/statline/#/CBS/nl/dataset/81302ned/table?fromstatweb. (Accessed 10 July 2023).

Choi, W.J., Arshad, M.A., Chang, S.X., Kim, T.H., 2006. Grain 15N of crops applied with organic and chemical fertilizers in a four-year rotation. Plant Soil 284, 165–174. https://doi.org/10.1007/s11104-006-0038-8.

De Carvalho, D.R., Bernardo, C., Alves, M., Flecker, A.S., Sparks, J.P., Moreira, M.Z., Santos Pompeu, P., 2020. Using δ 15 N of periphyton and fish to evaluate spatial and seasonal variation of anthropogenic nitrogen inputs in a polluted Brazilian river basin. Ecol. Indic. 115, 106372 https://doi.org/10.1016/j.ecolind.2020.106372.

De Vries, W., Kros, J., Oenema, O., De Klein, J., 2003. Uncertainties in the fate of nitrogen II: a quantitative assessment of the uncertainties in major nitrogen fluxes in the Netherlands. Nutr. Cycl. Agroecosyst. 66, 71–102.

Díaz-Álvarez, E.A., Lindig-Cisneros, R., De La Barrera, E., 2018. Biomonitors of atmospheric nitrogen deposition: potential uses and limitations. Conserv. Physiol. 6, coy011 https://doi.org/10.1093/conphys/coy011.

Elliott, E.M., Yu, Z., Cole, A.S., Coughlin, J.G., 2018. Isotopic advances in understanding reactive nitrogen deposition and atmospheric processing. Sci. Total Environ. 662, 393–403. https://doi.org/10.1016/j.scitotenv.2018.12.177.

Erisman, J., Bleeker, A., Galloway, J., Sutton, M., 2007. Reduced nitrogen in ecology and the environment. Environ. Pollut. 150, 140–149. https://doi.org/10.1016/j.envpol.2007.06.033.

Finlay, J.C., Kendall, C., 2007. Stable isotope tracing of temporal and spatial variability in organic matter sources to freshwater ecosystems. In: Michener, R., Lajtha, K. (Eds.), Stable Isotopes in Ecology and Environmental Science. Blackwell Publishing Ltd. https://doi.org/10.1002/9780470691854.ch10

Galloway, J.N., Aber, J.D., Erisman, J.W., Seitzinger, S.P., Howarth, R.W., Cowling, E.B., Cosby, B.J., 2003. The nitrogen cascade. Bioscience 53, 341–356. https://doi.org/10.1641/0006-3568(2003)053[0341:TNC]2.0.CO;2.

Ge, X.R., Schaap, M., De Vries, W., 2023. Improving spatial and temporal variation of ammonia emissions for the Netherlands using livestock housing information and a Sentinel-2-derived crop map. Atmos. Environ. X 17. https://doi.org/10.1016/j.aeaoa.2023.100207.

Gökçe, D., 2016. Algae as an indicator of water quality. In: Thajuddin, N., Dhanasekaran, D. (Eds.), Algae - Organisms for Imminent Biotechnology. IntechOpen, Rijeka. https://doi.org/10.5772/62916.

Hickman, J.E., Andela, N., Tsigaridis, K., Galy-Lacaux, C., Ossohou, M., Dammers, E., Van Damme, M., Clarisse, L., Bauer, S.E., 2021. Continental and ecoregion-specific drivers of atmospheric NO2 and NH3 seasonality over Africa revealed by satellite observations. Glob. Biogeochem. Cycles 35. https://doi.org/10.1029/2020GB006916.

Humphreys, J., Lan, R., Tao, S., 2021. Development and recent progress on ammonia synthesis catalysts for Haber–Bosch process. Adv. Energy Sustain. Res. 2, 1–23. https://doi.org/10.1002/AESR.202000043.

Koninklijk Nederlands Meteorologisch Instituut ('KNMI'), 2023. Windrozen van de Nederlandse hoofdstations [WWW Document].

Maberly, S.C., Van de Waal, D.B., Raven, J.A., 2022. Phytoplankton growth and nutrients. In: Encyclopedia of Inland Waters, , Second edition2, pp. 130–138. https://doi.org/10.1016/B978-0-12-819166-8.00111-0.

Malagó, A., Bouraoui, F., 2021. Global anthropogenic and natural nutrient fluxes: from local to planetary assessments. Environ. Res. Lett. 16 https://doi.org/10.1088/1748-9326/abe95f.

Markert, B., Wünschmann, S., 2011. Bioindicators and biomonitors: use of organisms to observe the influence of chemicals on the environment. In: Peter, Schröder, Collins, C.D. (Eds.), Organic Xenobiotics and Plants: From Mode of Action to Ecophysiology. Springer, Netherlands, Dordrecht, pp. 217–236. https://doi.org/10.1007/978-90-481-9852-8_10.

Martin, S.L., Hayes, D.B., Kendall, A.D., Hyndman, D.W., 2016. The land-use legacy effect: towards a mechanistic understanding of time-lagged water quality responses to land use/cover. Sci. Total Environ. 579, 1794–1803. https://doi.org/10.1016/j.scitotenv.2016.11.158.

Mooney, T.J., Pease, C.J., Hogan, A.C., Trenfield, M., Kleinhenz, L.S., Humphrey, C., van Dam, R.A., Harford, A.J., 2019. Freshwater chronic ammonia toxicity: a tropical-to-temperate comparison. Environ. Toxicol. Chem. 38, 177–189. https://doi.org/10.1002/ETC.4313.

Nieuwenhuis, H.S., Schokking, F., 1997. Land subsidence in drained peat areas of the Province of Friesland, The Netherlands. Q. J. Eng. Geol. 30, 37–48. https://doi.org/10.1144/GSL.QJEGH.1997.030.P1.04.

Nijssen, M., De Vries, M., Siepel, H., 2017. Pathways for the effects of increased nitrogen deposition on fauna. Biol. Conserv. 212, 423–431. https://doi.org/10.1016/j.biocon.2017.02.022.

Oenema, O., Van Liere, L., Schoumans, O., 2005. Effects of lowering nitrogen and phosphorus surpluses in agriculture on the quality of groundwater and surface water in the Netherlands. J. Hydrol. (Amst.) 304, 289–301. https://doi.org/10.1016/j.jhydrol.2004.07.044.

Oishi, Y., 2023. Seasonal differences in nitrogen deposition affect nitrogen content in mosses: implications for biomonitoring. Environ. Nanotechnol. Monit. Manag. 20, 100783 https://doi.org/10.1016/j.enmm.2023.100783.

Pinheiro, J.C., Bates, D.M., 2000. Mixed-effects Models in S and S-PLUS. Stat Comput.

Ritzema, H.P., Stuyt, L.C.P.M., 2015. Land drainage strategies to cope with climate change in the Netherlands. Acta Agric. Scand. Sect. B Soil Plant Sci. 65, 80–92. https://doi.org/10.1080/09064710.2014.994557.

Schulte-Uebbing, L.F., Beusen, A.H.W., Bouwman, A.F., de Vries, W., 2022. From planetary to regional boundaries for agricultural nitrogen pollution. Nature 610, 507–512. https://doi.org/10.1038/s41586-022-05158-2.

Shen, J., Chen, D., Bai, M., Sun, J., Coates, T., Lam, S.K., Li, Y., 2016. Ammonia deposition in the neighbourhood of an intensive cattle feedlot in Victoria, Australia. OPEN Sci. Rep. 6 https://doi.org/10.1038/srep32793.

Tang, Y.S., Stephens, A., Poskitt, J., Centre for Ecology & Hydrology, 2017. CEH ALPHA Sampler Instructions.

Toda, H., Uemura, Y., Okino, T., Kawanishi, T., Kawashima, H., 2002. Use of nitrogen stable isotope ratio of periphyton for monitoring nitrogen sources in a river system. Water Sci. Technol. 46, 431–435. https://doi.org/10.2166/WST.2002.0774.

Van Puijenbroek, P.J.T.M., Cleij, P., Visser, H., 2014. Aggregated indices for trends in eutrophication of different types of fresh water in the Netherlands. Ecol. Indic. 36, 456–462. https://doi.org/10.1016/j.ecolind.2013.08.022.

Vokhshoori, N.L., McCarthy, M.D., 2014. Compound-specific δ15N amino acid measurements in littoral mussels in the California upwelling ecosystem: a new approach to generating baseline δ15N isoscapes for coastal ecosystems. PLoS One 9. https://doi.org/10.1371/journal.pone.0098087.

Von Schiller, D., Euge, E., Arti, E.M., Arti, A., Llui, J.L., Riera, L., Fra, A., Sabater, N., Sant, C., 2007. Effects of nutrients and light on periphyton biomass and nitrogen uptake in Mediterranean streams with contrasting land uses. Freshw. Biol. 52, 891–906. https://doi.org/10.1111/j.1365-2427.2007.01742.x.

Wu, Yonghong, 2017. Periphyton and Its Study Methods. In: Periphyton: Functions and Application in Environmental Remediation. Elsevier, 1016/B978-0-12-801077-8.00001-6.

Yu, Q., Chen, Y., Ye, X., Zhang, Q., Zhang, Z., Tian, P., 2007. Evaluation of nitrification inhibitor 3,4-dimethyl pyrazole phosphate on nitrogen leaching in undisturbed soil columns. Chemosphere 67, 872–878. https://doi.org/10.1016/J.CHEMOSPHERE.2006.11.016.

Zhao, Y., Xiong, X., Wu, C., Xia, Y., Li, J., Wu, Y., 2017. Influence of light and temperature on the development and denitrification potential of periphytic biofilms. Sci. Total Environ. 613–614, 1430–1437. https://doi.org/10.1016/j.scitotenv.2017.06.117.